

Raman and Fourier transform infrared study of substitutional carbon incorporation in rapid thermal chemical vapor deposited $\text{Si}_{1-x-y}\text{Ge}_x\text{C}_y$ on (1 0 0) Si

Joanna Wasyluk,¹ Tatiana S. Perova,^{1,a)} and Francoise Meyer²

¹Department of Electronic and Electrical Engineering, University of Dublin, Trinity College, Dublin 2, Ireland

²Institut d'Électronique Fondamentale, CNRS URA 22, Bât. 220, Université Paris Sud, Orsay Cedex 91405, France

(Received 26 August 2009; accepted 5 December 2009; published online 27 January 2010)

We report on a detailed study of the dependence of the vibrational modes in rapid thermal chemical vapor deposited $\text{Si}_{1-x-y}\text{Ge}_x\text{C}_y$ films on the substitutional carbon concentration. $\text{Si}_{1-x-y}\text{Ge}_x\text{C}_y$ films were investigated using Raman and infrared spectroscopy with x varying in the range of 10%–16% and y in the range of 0%–1.8%. The introduction of C into thin SiGe layers reduces the average lattice constant. It has been shown that the integrated infrared intensity of the Si–C peak and the ratio of both the Raman integrated and peak intensities of the Si–C peak (at $\sim 605\text{ cm}^{-1}$) to the Si–Si peak of SiGeC layer, increase linearly with C content and are independent of the Ge content. This leads to the conclusion that infrared absorption and Raman scattering data can be used to determine the fraction of substitutional carbon content in $\text{Si}_{1-x-y}\text{Ge}_x\text{C}_y$ layers with a Ge content of up to 16%. It is also shown that the intensity ratio of the carbon satellite peak to the local carbon mode increases linearly with C content up to a C level of 1.8%. This confirms a conclusion of an increase in the probability of creating third-nearest-neighbor pairs with increasing carbon content, as derived from theoretical calculations. © 2010 American Institute of Physics. [doi:10.1063/1.3284937]

I. INTRODUCTION

The introduction of C into $\text{Si}_{1-x}\text{Ge}_x$ layers heteroepitaxially grown on Si has attracted considerable attention. It may have application to the fabrication of novel heterostructure devices using Si-based technology. This enables band engineering via strain control in group IV semiconductors.^{1,2} As shown recently, the addition of modest amounts of substitutional carbon into $\text{Si}_{1-x}\text{Ge}_x$ reduces the strain originating from the lattice mismatch between SiGe and Si and provides an additional design parameter in manipulating electronic properties.^{3,4} The presence of carbon in the SiGeC lattice induces a very large local bond distortion, resulting in a significant change in the phonon frequencies. Determination of the exact amount of substitutional carbon in alloys is not trivial, as the parameters of the vibrational bands, viz., peak position, linewidth, and intensity, are strongly dependent on the carbon content. A measurement of the vibrational C local mode at $\sim 605\text{ cm}^{-1}$ can be used to quantify the amount of substitutional carbon in $\text{Si}_{1-x-y}\text{Ge}_x\text{C}_y$ since it originates only from substitutional carbon. This measurement can also be used to estimate the amount of ordered carbon pairs versus randomly distributed carbon atoms. A number of recent publications^{5–12} were devoted to a study of the mechanism of the carbon distribution and ordering during $\text{Si}_{1-x-y}\text{Ge}_x\text{C}_y$ growth and the microscopic strains in $\text{Si}_{1-x-y}\text{Ge}_x\text{C}_y$ alloys with respect to the average lattice constant. There are a variety of interpretations in the literature on the origin of the

Raman satellite Si–C peak at $\sim 630\text{ cm}^{-1}$. Rowell *et al.*¹³ assigned this peak to the carbon on the nonsubstitutional sites, while Guedj *et al.*¹² and Rücker *et al.*,¹⁴ showed, by combining theoretical and experimental results, that the satellite Si–C peak corresponds to the third-nearest-neighbor (3nn) carbon pairs.

To date, no completely satisfactory experimental methods exist for the extraction of information on the fraction of the substitutional carbon from the total carbon content in SiGeC films with varying Ge content.

A discrepancy exists in the literature regarding the frequency behavior of Si–Si and Si–Ge vibrational bands in Raman spectroscopy as a function of C content. This is partly due to the limited number of investigations that have been performed on SiGeC structures. For instance, a decreasing dependence of the Si–Si peak with C content was experimentally observed in Refs. 7 and 18. Rücker and Methfessel²² predicted a negative shift in the Si–Si peak for SiGeC alloys using theoretical calculations. Rowell *et al.*¹³ did not find any systematic trend in the variation of the frequencies of Si–Si and Si–Ge peaks with changing C content.

Measurements by Melendez-Lira *et al.*¹⁰ showed a positive shift in the Si–Si peak with increasing C concentration. In Ref. 10, an increase in the Si–Ge peak with C content is also observed. However, the opposite trend in the Si–Ge peak frequency versus C content was obtained in this work. Differences in the behavior of the Si–Si and Si–Ge peak are discussed in this work in the context of the sample properties.

Contradictions also exist in the literature regarding

^{a)}Author to whom correspondence should be addressed. Tel.: +353 1 896 1432. FAX: +353 1 677 2442. Electronic-mail: perovat@tcd.ie.

changes in the frequency and in the intensity of the Si–C bands as a result of the addition of substitutional carbon. An increase in both intensity and frequency for both satellite and local Si–C modes was observed by Finkman *et al.*⁸ Whereas, in Ref. 13, it was shown that the frequency of the Si–C local mode at $\sim 605\text{ cm}^{-1}$ decreases with C content.

In this article, we report on a more detailed study of the carbon concentration dependence of the infrared and Raman modes in rapid thermal chemical vapor deposited (RTCVD) grown $\text{Si}_{1-x-y}\text{Ge}_x\text{C}_y$ samples with different x and y fractions varied over a small range. We present also a new approach to the calibration of optical methods for the extraction of the substitutional carbon concentration in SiGeC layers with carbon concentrations of up to 1.8%.

II. EXPERIMENTAL

A. Sample description

The samples were grown on (100) n -type Si substrates using a RTCVD deposition reactor. The layers were obtained using silane, germane, and methylsilane as precursors in a hydrogen carrier gas. Growth was performed at low temperature and reduced pressure, typically $550\text{ }^\circ\text{C}$ and 1 Torr, respectively. Four series of samples with different Ge and C content were studied: four samples with a Ge concentration of $\sim 16\%$ and carbon concentrations varying from 0% to 1.8% (first set, SX), three samples with a Ge concentration of $\sim 13.5\%$ and carbon concentrations varying from 0% to 1.7% (second set, X09), three samples with Ge concentrations of $\sim 9\%$ – 10% and carbon concentrations varying from 0% to 1.8% (third set, XX05), and five samples with Ge concentrations of $\sim 10\%$ and carbon concentrations varying from 0% to 1.25% (fourth set, 1003/X). The sample thickness varied from 500 to 1100 Å. Table I presents the structural parameters of these samples. More details on sample growth and characterization are given in Ref. 15. The Ge content was determined from Rutherford backscattering spectroscopy (RBS) data and the substitutional C concentration was obtained by x -ray diffraction (XRD) measurements (see Ref. 16 for details).

B. Infrared and Raman measurements

Fourier transform infrared (FTIR) measurements on $\text{Si}_{1-x-y}\text{Ge}_x\text{C}_y$ films were performed using normal incidence of light using a Digilab FTS 6000 spectrometer with a Globar source, a KBr beam splitter, and a mercury cadmium telluride detector. Due to the small size of samples, a micro-sampling Perkin–Elmer attachment was used for measurements, allowing the infrared beam to be focused to a spot size of ~ 3 – 5 mm in diameter.

Raman spectra were registered in backscattering geometry using a micro-Raman Renishaw 1000 system equipped with a Leica microscope. An 1800 lines/mm grating was used for all measurements, providing a spectral resolution of $\sim 1\text{ cm}^{-1}$. As an excitation source, the 514 nm line of an Ar⁺ laser with a power of 10 mW was used. The laser spot was focused on the sample surface using a $50\times$ objective. The infrared and Raman spectra obtained were analyzed using a mixture of Gaussian and Lorentzian peak fitting functions.

TABLE I. Structural parameters of the $\text{Si}_{1-x-y}\text{Ge}_x\text{C}_y$ thin films.

Sample	Ge content $x\%$ (by RBS)	C content $y\%$ (by XRD)	Thickness of SiGeC layer (Å)
Set 1 (SX)			
S1	16	0	700
S2	16	0.5	1000
S3	16	1.1	1000
S4	16	1.8	1000
Set 2 (X09)			
309	13.5	0	800
409	13.5	1.1	1000
509	13.5	1.7	800
Set 3 (XX05)			
1105	9	0	500
805	9.5	1.2	570
1005	10	1.8	530
Set 4 (1003/X)			
1003/1	10.5	0	1080
1003/2	9.7	0.35	1550
1003/3	9.6	0.7	1550
1003/4	10.2	1.1	1040
1103	10.2	1.25	1100

III. RESULTS AND DISCUSSION

A. FTIR results

The infrared absorption spectra of the SiGeC layer exhibit a Si–C vibrational band at 605 cm^{-1} . This band has a very small intensity from the SiGeC layers with a low carbon concentration ($\sim 1\%$ – 2%). In addition, this band is overlapped by an intense Si–Si phonon band from the Si crystalline lattice at 614 cm^{-1} . For these reasons, quantitative analysis of the band at 605 cm^{-1} becomes complicated. The spectra of the reference samples, that is, SiGe layers with no carbon, were subtracted from the spectra of samples containing C in order to remove the contribution of vibrational bands other than those attributed to carbon from the spectra corresponding to the $\text{Si}_{1-x-y}\text{Ge}_x\text{C}_y$ film. The region between 750 and 800 cm^{-1} was also monitored for a peak assignable to the Si–C stretching vibration. No absorption peak at $\sim 800\text{ cm}^{-1}$ was observed for any of the measured SiGeC samples, indicating the absence of SiC precipitates.¹⁷

The infrared absorption spectra obtained after subtraction for the first set of samples are shown in Fig. 1 as an example. The spectral feature near $\sim 605\text{ cm}^{-1}$ is due to the Si–C local mode stretching vibration of the substitutional carbon. A full width at half maximum of about 20 cm^{-1} is observed from the SiGeC sample with a low carbon concentration. The linewidth of the Si–C peak increases asymmetrically to higher energies with increasing carbon concentration, due to a presence of the satellite peak at $\sim 625\text{ cm}^{-1}$ (Fig. 1). The dependence of the integrated intensity (A_{int}) of the Si–C peak on the substitutional C content (y) is shown in Fig. 2, allowing comparison with the results obtained by Finkman *et al.*¹⁸ for a set of samples with a Ge content of 10%. As can be seen from this figure, all four sets of samples investigated here fit the linear function

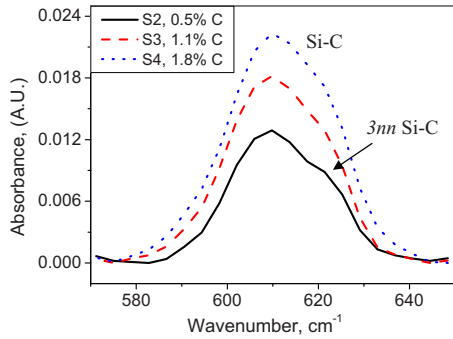


FIG. 1. (Color online) FTIR spectra for the first set of samples (SX) with a Ge content of 16% shown in the region of the Si–C band at ~ 605 cm^{-1} .

$$A_{\text{int}} = 0.39y, \quad (1)$$

which is independent of the Ge content. The linear fit obtained differs only slightly from the linear dependence $A_{\text{int}} = 0.34y$, obtained by Finkman *et al.*¹⁸ Therefore, we conclude that the intensity of the infrared Si–C vibrational band can indeed be used for the determination of the C content in the substitutional sites for SiGeC layers.

B. Raman results

Raman scattering offers an advantage over infrared absorption in that no absolute intensity measurements are required. This is because the intensity of the Si–C Raman peak at 605 cm^{-1} can be compared with the intensity of the Si–Si peak near 520 cm^{-1} (the Si–Si mode is infrared forbidden). The Raman spectrum of the $\text{Si}_{1-x-y}\text{Ge}_x\text{C}_y$ layer structure is composed of four distinct features, identified as the Ge–Ge (200 – 300 cm^{-1}), Si–Ge (350 – 450 cm^{-1}), Si–Si (~ 520 cm^{-1}), and Si–C (600 – 650 cm^{-1}) vibrations (see Fig. 3). Due to the small film thickness, the dominant peak in the spectrum is the Si–Si vibrational mode from the substrate. In the same manner used for the infrared data, the spectra of SiGe layers without carbon were used as references for subtraction from the SiGeC sample spectrum.

Figure 4 shows the spectra of samples $\text{Si}_{0.887}\text{Ge}_{0.095}\text{C}_{0.018}$ and $\text{Si}_{0.893}\text{Ge}_{0.095}\text{C}_{0.012}$, with the Si–C vibrational mode obtained after subtraction. Two Si–C peaks are seen (Fig. 4):

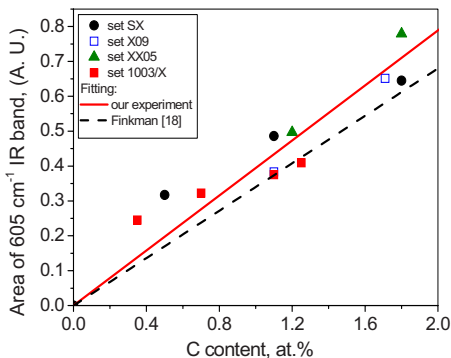


FIG. 2. (Color online) Integrated intensity of the Si–C infrared peak as a function of carbon content for all samples. Solid line is a linear fitting function $A_{\text{int}} = 0.39y$ to the experimental results obtained in this work. Dashed line is a linear fitting function $A_{\text{int}} = 0.34y$ obtained by Finkman *et al.* (Ref. 18) for one set of samples.

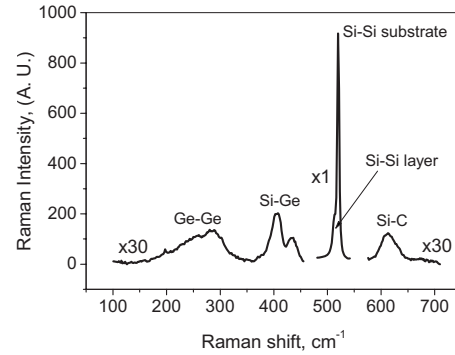


FIG. 3. Raman spectrum of sample S4 with $\text{Si}_{0.822}\text{Ge}_{0.16}\text{C}_{0.018}$ thin film deposited on (100) oriented Si substrate.

the main C local peak at ~ 605 cm^{-1} corresponds to substitutional carbon, and the satellite peak at ~ 630 cm^{-1} is assigned to a partial contribution from the 3nn configuration of C atoms.^{12,14}

Our results demonstrate that both of the peaks at ~ 605 and ~ 630 cm^{-1} change their position and intensity depending on the carbon concentration, y . There is a pronounced linear increase in the peak position of the satellite and local Si–C peak with concentration y (Fig. 5), which is in agreement with Refs. 18 and 21. Their dependence on the C content is

$$\omega_{\text{Si-C}} = 623.9 + 364.2y, \quad (2)$$

for the satellite peak, and

$$\omega_{\text{Si-C}} = 604.3 + 229.3y, \quad (3)$$

for the local peak. These results differ slightly from the linear dependence obtained in Ref. 18 because a larger number of samples with a wider range of Ge and C concentrations is analyzed in this present work. The deviation observed could also be due to different fitting procedures. The total intensity of the Si–C peaks increases with carbon content, which is in good agreement with previously published data.¹⁸ Figure 6 shows the ratio of the integrated intensities of the Si–C Raman peak (at ~ 605 cm^{-1}) to the Si–Si peak for the SiGeC layer, as a function of y . Data points are presented for all four sets of samples studied here and compared with previously published data on a set of samples with a Ge content of 10%.¹⁸ The ratio of the integrated intensities of the Si–C

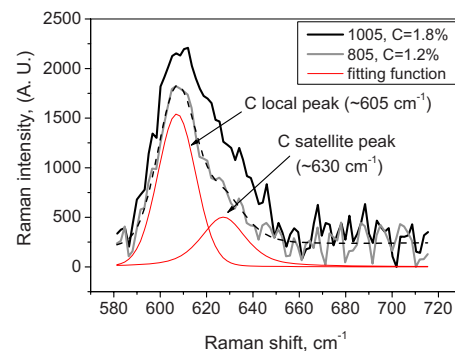


FIG. 4. (Color online) Raman spectra of samples 1005 and 805 shown in the region of the Si–C peaks. The dashed line shows the fitting of the spectrum for sample 805 with two functions (thin lines).

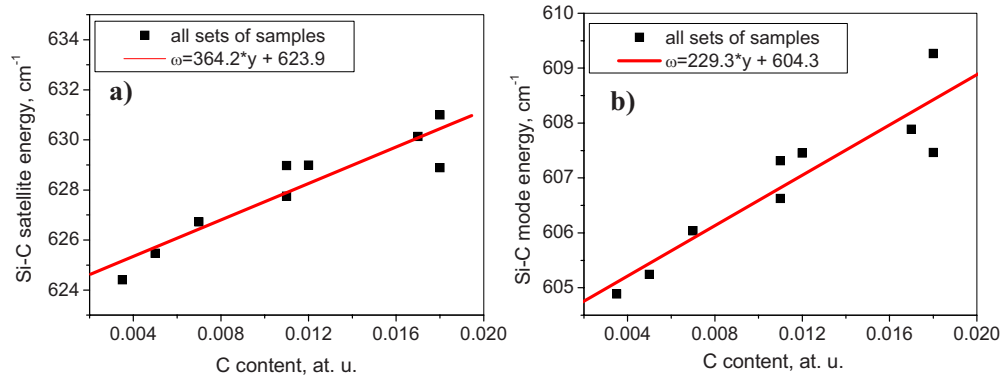


FIG. 5. (Color online) The Raman peak position of (a) the satellite C band and (b) the main C band for the sets of samples studied in this work.

Raman peak to the Si–Si peak of the $\text{Si}_{1-x-y}\text{Ge}_x\text{C}_y$ layer increases linearly with carbon content. The linear dependence $I(C_{\text{local}})/I(\text{Si–Si}_{\text{layer}})$ versus C content can be described by the following equation:

$$I(C)/I(\text{Si–Si}) = 0.0303y. \quad (4)$$

As can be seen from Fig. 6, a linear dependence for all sets of samples with different Ge concentration is in good agreement with previously published data for samples with a Ge concentration of approximately 10%,¹⁸ as well as with results obtained in Ref. 19 for SiC alloys with C contents of up to 0.4%. This leads to the conclusion that the dependence of $I(C_{\text{local}})/I(\text{Si–Si}_{\text{layer}})$ on y (with y in the range of 0%–1.8%) is unaffected by the Ge content. These results confirm that Raman spectroscopy can be used to determine substitutional carbon concentrations in the SiGeC layer with Ge concentrations of up to 16% and C up to 1.8%.

The dependence of the peak intensity ratio of the Si–C Raman peak to the Si–Si peak of the $\text{Si}_{1-x-y}\text{Ge}_x\text{C}_y$ layer on y was also investigated. The experimental data are described by the linear function $I(C)/I(\text{Si–Si}) = 0.0117y$. It was found that the experimental results obtained for the peak intensities have a better linear fit than the integrated intensities. This could be due to the greater inaccuracies in determining the integrated intensity of Raman spectra with two overlapping peaks. As predicted from calculation,²² the presence of a satellite peak in the Raman spectrum is associated with ordered

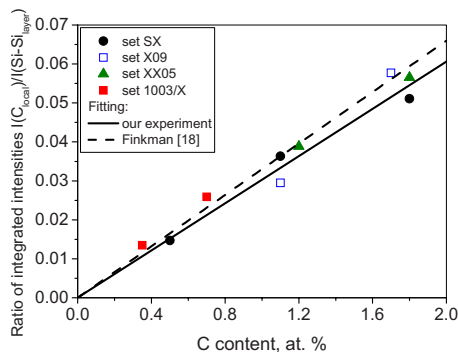


FIG. 6. (Color online) The ratio of the integrated intensities of the Si–C Raman peak to the Si–Si peak of the $\text{Si}_{1-x-y}\text{Ge}_x\text{C}_y$ layer as a function of substitutional carbon content. Solid line is a linear fitting function $I(C)/I(\text{Si–Si}) = 0.0303y$ to the results obtained in this work for all sets of samples. Dashed line is a linear fitting function $I(C)/I(\text{Si–Si}) = 0.033y$ to the results for one set of samples obtained in Ref. 18.

carbon pairs in substitutional sites. The intensity ratio of the carbon 3nn satellite peak to the total carbon-local-mode as a function of C content up to 1.8% is shown in Fig. 7. The ratio increases with carbon content as the probability of creating 3nn pairs increases, which is in agreement with the results obtained in Ref. 18. The carbon pair is most strongly bound at the 3nn coordination. This configuration is the one most preferred by carbon atoms as for this geometry the short Si–C bonds can be accommodated easily without strong bond-bending distortion.¹⁴

Despite the absence of data points for C concentrations $< 0.35\%$, the experimental data were fitted with a linear function based on the fact²⁰ that for total carbon concentrations of up to 1%, carbon atoms predominantly sit on substitutional sites. This enables us to consider that the ratio of the carbon 3nn satellite peak to the total carbon-local-mode equals zero in the absence of substitutional carbon in the SiGeC layer. We believe that the deviation of the experimental data from the linear function is due to the fact that fitting the Raman spectra with two curves is not very accurate, particularly at low carbon concentrations.

In this study, a reduction in the frequency of the Si–Si peak with increasing C content was observed for all sample sets. This is in agreement with data obtained in Refs. 7 and 18 for SiGeC samples as well as in Ref. 21 for SiC layers. Figure 8 shows the Raman peak position of the Si–Si mode of the SiGeC layers, for two sets of samples (XX05 and 1003/X) with approximately the same Ge content ($\sim 10\%$), as a function of C content. The Si–Si peak from the SiGeC

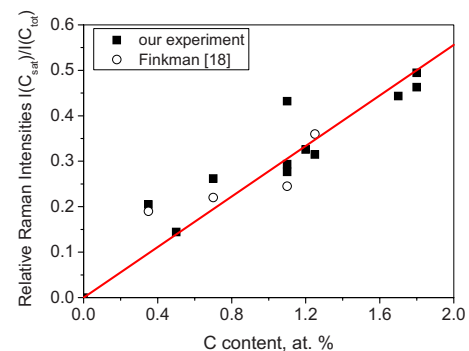


FIG. 7. (Color online) Raman peak intensities ratio of the carbon satellite peak $[I(C_{\text{sat}})]$ to the total intensity $[I(C_{\text{tot}})]$ of the carbon-local mode as a function of y .

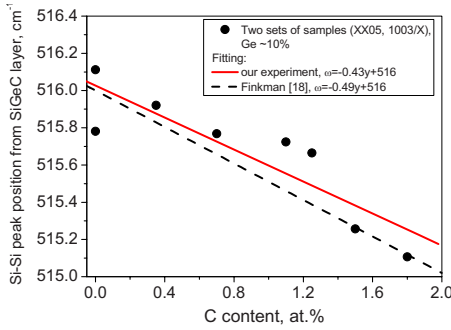


FIG. 8. (Color online) Raman peak position of the Si-Si mode of the $\text{Si}_{0.9-y}\text{Ge}_{0.10}\text{C}_y$ layer as a function of C content. Solid line is a fitting function to our experiment. Dashed line is a fitting function for the data from Finkman *et al.* (Ref. 18).

layer shifts to lower wave numbers with increasing C concentration. The linear relationship obtained in this work is in agreement with results obtained earlier for one set of samples.¹⁸ However, different linear dependencies of $\omega_{\text{Si-Si}}$ on C content are observed for samples with a different Ge concentration. For the set of samples with 16% Ge content, the dependence of the Si-Si peak on the C content is described by the function $\omega_{\text{Si-Si}} = -0.95y + 514.4$, while for the set of samples with 13.5% Ge content, the experimental data are fitted to the function $\omega_{\text{Si-Si}} = -0.75y + 514.9$.

As expected, the shift in the Si-Si mode from the SiGeC layer depends on the Ge content. The Si-Si peak positions for samples with different Ge content are presented in Table II. As can be seen from Fig. 8, and also from Table II, the increase in Ge content in the $\text{Si}_{1-x-y}\text{Ge}_x\text{C}_y$ layer shifts the Si-Si phonon peak to lower frequencies. This is in agreement with theoretical calculations performed in Refs. 7 and 22.

The dependencies of the Si-Ge peak shift ($\Delta\omega_{\text{Si-Ge}}$) versus carbon content for different sets of SiGeC samples are shown in Fig. 9. $\Delta\omega_{\text{Si-Ge}}$ is the experimental Raman shift between the position of the Si-Ge peak from the SiGeC layer and the Si-Ge peak for the SiGe layers. Different linear dependencies of the Si-Ge peak versus C content were obtained from different sets of samples with Ge contents $\sim 10\%$, 13.5% , and 16% (see Fig. 9). For low Ge content, around $\sim 10\%$, an increase in the shift, $\Delta\omega_{\text{Si-Ge}}$, with increasing carbon content is observed. For the SiGeC layer with Ge content $\sim 13.5\%$ we observe the opposite behavior in the Si-Ge peak position. $\Delta\omega_{\text{Si-Ge}}$ only slightly decreases with C content. For higher Ge content, $x \approx 16\%$, the shift in the Si-Ge peak decreases faster with the addition of carbon than for SiGeC layers with a Ge content around $\sim 13.5\%$. A similar analysis of the compositional dependence $\Delta\omega_{\text{Si-Ge}}(y)$ with carbon content was performed in Ref. 10 for SiGeC layers

TABLE II. The Si-Si peak position of $\text{Si}_{1-x}\text{Ge}_x$ and $\text{Si}_{1-x-0.01}\text{Ge}_x\text{C}_{0.01}$ thin films with different Ge content.

Ge content (%)	Si-Si peak position of $\text{Si}_{1-x}\text{Ge}_x$ (cm^{-1})	Si-Si peak position of $\text{Si}_{0.989-x}\text{Ge}_x\text{C}_{0.011}$ (cm^{-1})
~ 10	516.1	515.78
13.5	514.9	514.4
16	514.4	513.35

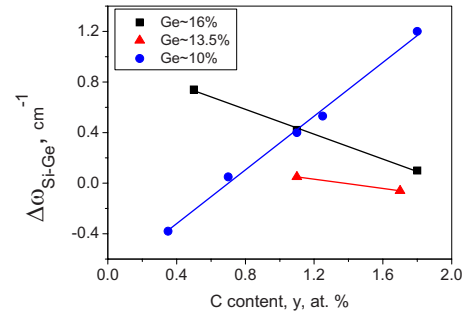


FIG. 9. (Color online) Raman shift in the Si-Ge mode of the SiGeC layers as a function of carbon content. $\Delta\omega_{\text{Si-Ge}}$ is the Raman shift between the peak position of the Si-Ge phonon mode for SiGeC layer and the Si-Ge mode for SiGe layers.

with a substitutional carbon content up to 0.5% and a Ge content around $\sim 20\%$ and $\sim 50\%$. As shown in Ref. 10, $\Delta\omega_{\text{Si-Ge}}(y)$ increases with increasing carbon content for a SiGeC layer with Ge content up to 50%. However, if one considers only the data points for Ge content around 20%, the decrease of $\Delta\omega_{\text{Si-Ge}}(y)$ versus C content is clearly seen from Fig. 3 in Ref. 10. This agrees with our experimental results obtained for SiGeC layers with Ge content, $x \approx 16\%$. The behavior of Ge-Ge peak was not considered in this work due to the low Ge content (up to 16%) in the SiGeC alloys under investigation. It has an effect on the Ge-Ge peak, but the effect is not large enough for reliable analysis.

The composition and strain dependence of the Si-Si phonon energies in $\text{Si}_{1-x}\text{Ge}_x$ layers is also analyzed in this work. For small values of strain, the frequency of the Si-Si peak can be described by the expression given by Tsang *et al.*,²³

$$\omega_{\text{Si-Si}} = 520 - 68x + \Delta\omega_{\text{Si-Si}}, \quad (5)$$

where $\omega_{\text{Si-Si}}$ is the experimental Si-Si peak position of the $\text{Si}_{1-x}\text{Ge}_x$ layer and x is the Ge content. The term $68x$ describes the compositional shift in a fully relaxed film and the last term $\Delta\omega_{\text{Si-Si}}$ describes the shift in the Si-Si peak due only to strain. $\Delta\omega_{\text{Si-Si}}$ is the frequency shift between the Si-Si peak position measured experimentally from the $\text{Si}_{1-x}\text{Ge}_x$ film and the calculated frequency of the Si-Si peak for a fully relaxed $\text{Si}_{1-x}\text{Ge}_x$ layer. It is well known, that for small values of strain, the shift in the Si-Si phonon energy is linear with strain, ε

$$\Delta\omega_{\text{Si-Si}} = -p_{\text{Si}}\varepsilon(x), \quad (6)$$

where p_{Si} is a strain phonon coefficient. $\varepsilon(x)$ is obtained from the lattice mismatch between the SiGe alloy and the Si substrate

$$\varepsilon(x) = [a(\text{Si}) - a_{\text{rel}}(\text{Si}_{1-x}\text{Ge}_x)]/a_{\text{rel}}(\text{Si}_{1-x}\text{Ge}_x). \quad (7)$$

$a(\text{Si})$ is the lattice constant of Si (5.43 \AA) and $a_{\text{rel}}(\text{Si}_{1-x}\text{Ge}_x)$ is the lattice constant of the relaxed $\text{Si}_{1-x}\text{Ge}_x$ alloy with the appropriate composition. The calculated values of $\varepsilon(x)$, $\Delta\omega_{\text{Si-Si}}$ and the constant p_{Si} are presented in Table III. The value of the constant p_{Si} varies from 720 to 850 cm^{-1} for SiGe layers with Ge content in the range of $\sim 10\%$ – 16% . After fitting a linear function to our data, we obtained the average value of the strain phonon coefficient, p_{Si}

TABLE III. The lattice constant, strain, Si–Si peak position, and strain phonon coefficient for Si_{1-x}Ge_x layers.

Samples	$a_{\text{SiGe}}(x)$ (Å)	$\varepsilon(x)$	$\omega_{\text{Si-Si}}$ for relaxed SiGe layer (cm ⁻¹)	$\omega_{\text{Si-Si}}$ experimental value (cm ⁻¹)	$\Delta\omega_{\text{Si-Si}}$ (cm ⁻¹)	p_{Si} (cm ⁻¹)
Si _{0.84} Ge _{0.16}	5.4636	-0.00615	509.12	514.33	-5.21	847
Si _{0.865} Ge _{0.135}	5.45835	-0.00519	510.82	514.87	-4.05	781
Si _{0.903} Ge _{0.097}	5.45037	-0.00374	513.40	516.11	-2.71	725
Si _{0.895} Ge _{0.105}	5.45205	-0.00404	512.86	515.78	-2.92	722

=790 cm⁻¹. This value is in very good agreement with the calculation performed by Rücker and Methfessel²² and it does not differ greatly from the value of ~830 cm⁻¹ obtained experimentally by Tsang *et al.*²³ for SiGe layers with Ge content <50%, and p_{Si} calculated theoretically in Refs. 24 and 25. Values of $p_{\text{Si}}=730\pm 70$ cm⁻¹ were most recently obtained by Pezzoli *et al.*²⁶ for SiGe alloys with a wide range of Ge content, which is also in good agreement with the value obtained in this work.

IV. CONCLUSION

A detailed study of Raman and infrared spectra of the Si_{1-x-y}Ge_xC_y layers with different Ge and C content was performed in order to gain a better understanding of carbon incorporation and its influence on SiGeC structures. An increase in the linewidth and intensity of the Si–C peaks with the carbon content was observed in both the infrared and Raman spectra, which is in agreement with previously published data, over a limited range of x and y .^{13,18} FTIR analysis shows that the integrated intensity of the Si–C peak increases linearly with the C concentration and is independent of the Ge content, at least up to 16%. In all the Raman experiments performed in this study, a linear dependence of the relative Raman intensity $I(C_{\text{local}})/I(\text{Si-Si}_{\text{layer}})$ versus C content of the SiGeC samples was obtained. The relative Raman intensities increase linearly with C content and they are independent of the Ge content up to 16%.

We conclude that both FTIR and Raman spectroscopy can be used as nondestructive analytical methods for the determination of the amount of substitutional carbon in SiGeC layers. However, since the Raman approach uses relative intensity measurements, it is far less dependent on the sample condition than traditional infrared methods. The satellite peak at ~630 cm⁻¹ has been observed in the Raman spectrum of all samples containing C, confirming the ordering of the C–C pairs during RTCVD layer growth. This is in accordance with both theoretical predictions²² and some experimental results^{8,18,19} obtained for SiGeC films (with lower Ge content) grown by molecular beam epitaxy and RTCVD techniques. It was shown that increasing the C and Ge content in the SiGeC lattice leads to a reduction in the frequency of the Si–Si mode. The frequency of both the satellite and local Si–C modes increases with C content. The Si–C absorption band at ~800 cm⁻¹ was not observed from any of samples studied here, indicating that there is no carbon in the SiC precipitate phase.

ACKNOWLEDGMENTS

J.W. acknowledges the financial support of IRCSET Ireland, Postgraduate Award. We also would like to thank Kévin Béranger for help with measurements and data analysis.

- ¹K. Eberl, S. S. Iyer, S. Zollner, J. C. Tsang, and F. K. LeGoues, *Appl. Phys. Lett.* **60**, 3033 (1992).
- ²P. Boucaud, C. Francis, F. H. Julien, J. M. Lourtioz, D. Bouchier, S. Bondar, B. Lambert, and J. L. Regolini, *Appl. Phys. Lett.* **64**, 875 (1994).
- ³A. R. Powell, K. Eberl, F. E. Legues, B. A. Ek, and S. S. Iyer, *J. Vac. Sci. Technol. B* **11**, 1064 (1993).
- ⁴H. J. Osten, E. Bugiel, and P. Zaumseil, *Appl. Phys. Lett.* **65**, 2559 (1994).
- ⁵J. L. Regolini, S. Bondar, J. C. Oberlin, F. Ferriou, M. Gauneau, B. Lambert, and P. Boucaud, *J. Vac. Sci. Technol. A* **12**, 1015 (1994).
- ⁶J. Boulmer, P. Boucaud, C. Guedj, D. Debarre, D. Bouchier, E. Finkman, S. Praver, K. Nugent, A. Desmur-Larre, C. Godet, I. Roca, and P. Cabarrocas, *J. Cryst. Growth* **157**, 436 (1995).
- ⁷J. Menéndez, P. Gopalan, G. S. Spencer, N. Cave, and J. W. Strane, *Appl. Phys. Lett.* **66**, 1160 (1995).
- ⁸E. Finkman, H. Rücker, F. Meyer, S. D. Praver, D. Bouchier, J. Boulmer, S. Bodnar, and J. L. Regolini, *Thin Solid Films* **294**, 118 (1997).
- ⁹M. Meléndez-Lira, J. D. Lorentzen, J. Menéndez, W. Windl, N. G. Cave, R. Liu, J. W. Christiansen, N. D. Theodore, and J. J. Candelaria, *Phys. Rev. B* **56**, 3648 (1997).
- ¹⁰M. Meléndez-Lira, J. Menendez, W. Windl, O. F. Sankey, G. S. Spencer, S. Segó, R. B. Culbertson, A. E. Bair, and T. L. Alford, *Phys. Rev. B* **54**, 12866 (1996).
- ¹¹H. Nitta, J. Tanable, M. Sakuraba, and J. Murota, *Thin Solid Films* **508**, 140 (2006).
- ¹²C. Guedj, X. Portier, A. Hairie, D. Bouchier, G. Calvarin, and B. Piriou, *Thin Solid Films* **294**, 129 (1997).
- ¹³N. L. Rowell, D. J. Lockwood, and J. M. Baribeau, *J. Appl. Phys.* **103**, 063513 (2008).
- ¹⁴H. Rücker, M. Methfessel, B. Dietrich, K. Pressel, and H. J. Osten, *Phys. Rev. B* **53**, 1302 (1996).
- ¹⁵S. Bodnar and J. L. Regolini, *J. Vac. Sci. Technol. A* **13**, 2336 (1995).
- ¹⁶M. Mamor, C. Guedj, P. Boucaud, F. Meyer, and D. Bouchier, *Mater. Res. Soc. Symp. Proc.* **379**, 137 (1995).
- ¹⁷J. W. Strane, H. J. Stein, S. R. Lee, B. L. Doyle, S. T. Picraux, and J. W. Mayer, *Appl. Phys. Lett.* **63**, 2786 (1993).
- ¹⁸F. Finkman, F. Meyer, and M. Mamor, *J. Appl. Phys.* **89**, 2580 (2001).
- ¹⁹M. Meléndez-Lira, J. Menendez, K. M. Kramer, M. O. Thompson, N. Cave, R. Liu, J. W. Christiansen, N. D. Theodore, and J. J. Candelaria, *J. Appl. Phys.* **82**, 4246 (1997).
- ²⁰J.-M. Baribeau, D. J. Lockwood, J. Balle, S. J. Rolfe, and G. I. Sproule, *Mater. Sci. Eng., B* **89**, 296 (2002).
- ²¹D. L. Lockwood, H. X. Xu, and J.-M. Baribeau, *Phys. Rev. B* **68**, 115308 (2003).
- ²²H. Rücker and M. Methfessel, *Phys. Rev. B* **52**, 11059 (1995).
- ²³J. C. Tsang, P. M. Mooney, F. Dacol, and J. O. Chu, *J. Appl. Phys.* **75**, 8098 (1994).
- ²⁴S. de Gironcoli, *Phys. Rev. B* **46**, 2412 (1992).
- ²⁵J. Zi, K. Zhang, and X. Xie, *Phys. Rev. B* **45**, 9447 (1992).
- ²⁶F. Pezzoli, E. Bonera, E. Grilli, M. Guzzi, S. Sanguinetti, D. Chrastina, G. Isella, H. von Kanel, E. Wintersberger, J. Stangl, and G. Bauer, *Mater. Sci. Semicond. Process.* **11**, 279 (2008).